The Vinyl Radical and Fluorinated Vinyl Radicals, $C_2H_{3-n}F_n$ ($n = 0-3$), and Corresponding Anions: Comparison with the Isoelectronic Complexes $[X\cdots YC\equiv CZ]^-$

Andrew C. Simmonett, Steven E. Wheeler, and Henry F. Schaefer III*

Center for Computational Chemistry, University of Georgia, Athens, Georgia 30602

Received: November 12, 2003

Density functional theory (DFT) has been utilized to study the vinyl radical and fluorinated vinyl radical series, $C_2H_{3-n}F_n$, $n = 0-3$. Six different functionals—B3LYP, B3P86, BHLYP, BLYP, BP86, and LSDA—were used. A double-ζ basis set, augmented with additional s- and p-type diffuse functions as well as additional polarization functions (DZP++), was employed for all of the computations. Extensive calibrative studies have demonstrated that the DZP++ B3LYP, BLYP, and BP86 methods do a good job in the prediction of electron affinities. Neutral-anion energy separations were used to calculate the adiabatic electron affinities (EA_{ad}), the vertical electron affinities (EA_{vert}), and the vertical detachment energies (VDE). These electron affinities were found to get progressively larger as the number of fluorines is increased; ZPVE-corrected values predicted by the reliable BLYP method are 0.66 eV (C_2H_3), 1.54 eV (C_2H_2F), 1.96 eV (C_2HF_2), and 2.40 eV (C_2F_3). This trend can be attributed to increasing anion stability, which can be rationalized in terms of inductive and negative hyperconjugative effects. Optimized geometries for all of the neutral and anionic species, which are indicative of the aforementioned effects, are presented. The 1-fluorovinyl radical is found to lie lowest in energy of the mono-fluorinated species, whereas the most stable anion of the same stoichiometry is a fluoride···acetylene complex, which is found to lie 19.5 kcal mol^{-1} lower than the 1-fluorovinyl anion using BLYP. The most stable configuration for the difluorinated species is 2,2-difluorovinyl for both the neutral radical and the anion.

I. Introduction

The vinyl radical and its fluorinated derivatives have been studied over recent decades, both theoretically[1−5] and experimentally.[1,6−14] The 70's and 80's saw the publication[3,5] of studies of both the vinyl and trifluorovinyl radicals, carried out using semiempirical methods or Hartree−Fock theory with minimal basis sets and focused on calculating the radicals' geometries and harmonic vibrational frequencies. The evolution of computers has enabled more elaborate levels of theory to be employed in more recent years, such as the recent paper by Goldschleger, Akimov, Misochko, and Wight,[1] which found excellent agreement between experimental and B3LYP predicted hyperfine coupling constants. A detailed study of the electronic transitions of the vinyl radical, computed at the MRCISD and CASSCF levels of theory was published recently by Zhang and Morokuma.[4] However, despite this interest, no systematic study of the effects of halogen substitution on the electronic properties of the vinyl radical has been published. Electron affinities (EAs) are extremely useful in thermochemistry[15−17] and have many roles in semiconductor technology.[18−21]

An earlier study,[22] somewhat surprisingly, showed that the electron affinities of halide-substituted methyl radicals do not necessarily correlate with the electronegativities of the different halide substituents. However, the authors found that substituting the hydrogen atoms with fluorine atoms increases the electron affinity of the species, as expected on simple electronegativity grounds. Given these results, one of the principal aims of this research is to extend this study to fluorinated vinyl radicals and to ascertain whether similar trends are observed.

In this discussion, the quantity EA_{ad} will be used to represent the adiabatic electron affinity, i.e., the electron affinity associated with a slow neutral-to-anion transition that allows geometric rearrangement to occur. In polyatomic systems, attachment of an electron is usually accompanied by a change in geometry, thus making adiabatic EAs difficult to measure experimentally. For this reason, both the vertical electron affinity (EA_{vert}) and the vertical detachment energy (VDE) are reported here, where these quantities correspond to the Franck−Condon transitions from the optimized anion to the neutral and from the optimized neutral to the anion, respectively. Assuming that the geometry of the species does not change drastically upon addition of an electron, the VDE and EA_{vert} provide lower and upper bounds, respectively, for the experimentally observed EAs. The experimental electron affinity should be close to the adiabatic value, should this change in geometry be small.

II. Theoretical Methods

The properties of the molecules were computed using six different DFT or hybrid HF/DFT functionals, defined below, with a DZP++ basis set. This basis set is comprised of the standard first row Huzinaga−Dunning double-ζ basis sets,[23,24] augmented with additional pure spherical harmonic polarization functions with $\alpha_d(C) = 0.75$, $\alpha_d(F) = 1.00$, and $\alpha_p(H) = 0.75$ and diffuse functions with $\alpha_s(C) = 0.04302$, $\alpha_p(C) = 0.03629$, $\alpha_s(F) = 0.1049$, $\alpha_p(F) = 0.0826$, and $\alpha_s(H) = 0.04415$. Spin unrestricted formulations of the DFT functionals were employed for the computation of the radicals' properties, as recommended by Pople, Gill, and Handy.[25]

The functionals used in this study are the following: (1) Becke's hybrid three-parameter exchange functional[26] (B3) with

---

* Corresponding author. E-mail: hfs@uga.edu.

10.1021/jp031240e CCC: $27.50

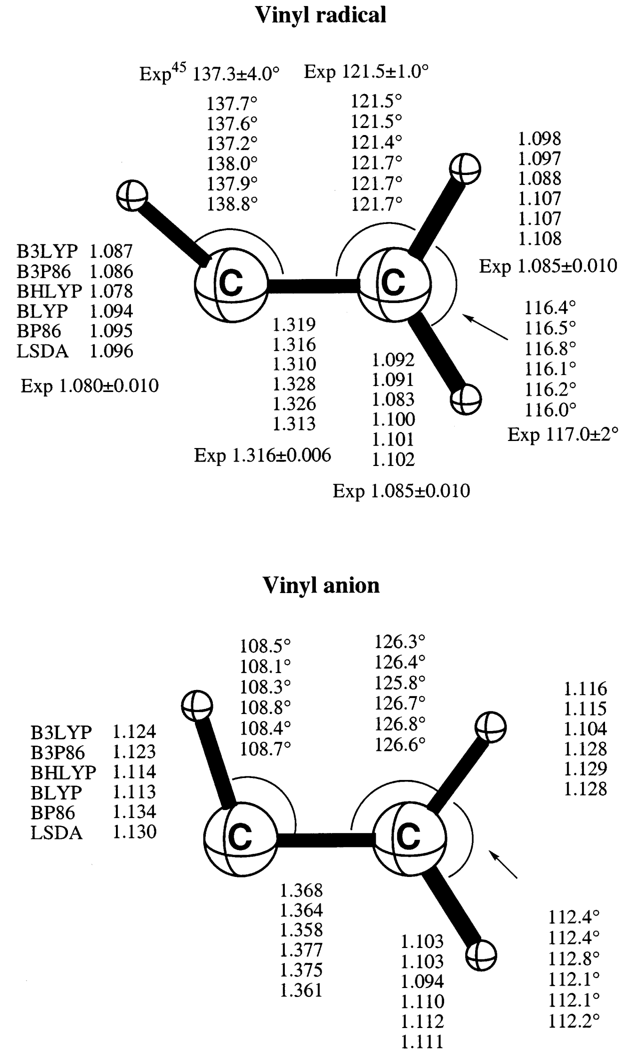

Figure 1. C_2H_3 and $C_2H_3^-$ bond lengths (Å) and angles.

Lee, Yang, and Parr's correlation functional[27] (LYP), designated as B3LYP; (2) the same B3 exchange functional with Perdew's 1986 correlation functional[28,29] (P86) giving the B3P86 hybrid functional; (3) Becke's half-and-half[30,31] correlation functional (BH) with the LYP exchange (BHLYP); (4) Becke's 1988 exchange functional[32] (B) with LYP correlation (BLYP); (5) the same B exchange functional with P86 correlation (BP86); and (6) the Slater exchange functional[33−35] (S) with Vosko, Wilk, and Nusair correlation[36] (VWN). This last functional uses the local spin density approximation and is, therefore, usually referred to as LSDA (this nomenclature has been adopted in this paper) but it may also be referred to as SVWN.

In a recent theoretical/experimental review,[2] Rienstra-Kiracofe, Tschumper, Schaefer, Nandi, and Ellison showed that DFT, when implemented with the same DZP++ basis set used here, has a tendency to overestimate EAs, with the exception of the BHLYP functional. The authors compared 91 experimentally measured EAs, each having an uncertainty of less than 0.09 eV, with DFT computed values. Of the six functionals mentioned above, B3LYP, BLYP, and BP86 were found to be the most consistently accurate with average absolute errors of 0.14 (0.16), 0.14 (0.15), and 0.18 (0.19) eV, respectively, where the values in parentheses represent the zero-point vibrational energy (ZPVE) corrected values. The corresponding absolute values of the maximum errors for these functionals were reported as 0.71 (0.76), 0.67 (0.71), and 0.62 (0.66) eV.

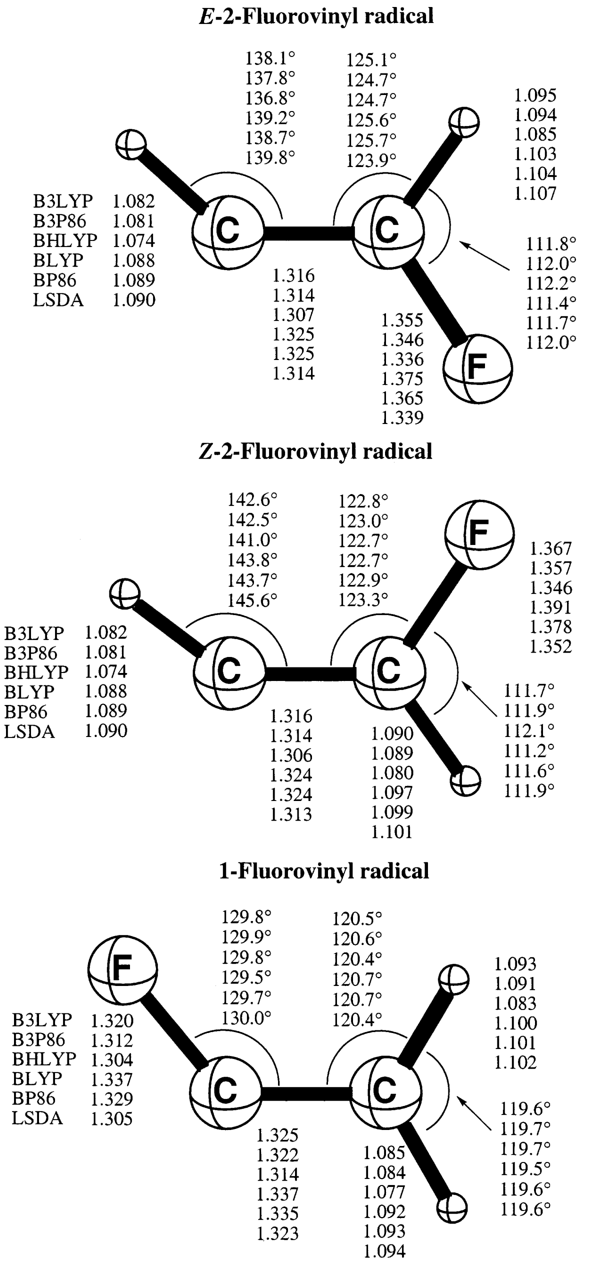

Figure 2. C_2H_2F bond lengths (Å) and angles.

For clarity, the quantities to be computed are explicitly defined below:

$$\mathrm{EA_{ad}} = E_{\text{(optimized neutral)}} - E_{\text{(optimized anion)}}$$

$$\mathrm{EA_{vert}} = E_{\text{(optimized neutral)}} - E_{\text{(anion at optimized neutral geometry)}}$$

$$\mathrm{VDE} = E_{\text{(neutral at optimized anion geometry)}} - E_{\text{(optimized anion)}}$$

All structures were optimized using analytic gradients, yielding stationary points that were characterized by computing harmonic vibrational frequencies. The structures presented were confirmed to be minima. Natural population analysis (NPA) computations were carried out at the B3LYP level of theory at the B3LYP optimized geometries. These facilitated a qualitative comparison of the "atomic charges" between neutral and anion species. All of the quantum chemical computations were carried out using the GAUSSIAN 94 software package.[37]

III. Results

We have computed optimized geometries and EAs for the vinyl radical and a series of fluorinated vinyl radicals. The aim

TABLE 1: Predicted EAs of the Vinyl Radical and Substituted Vinyl Radicals (in eV) (ZPVE corrected EA$_{ad}$ are in parentheses; EA$_{vert}$ and VDE are not corrected for ZPVE.)

	B3LYP	B3P86	BHLYP	BLYP	BP86	LSDA	Experiment
vinyl radical							0.668 ± 0.024[a]
EA$_{ad}$	0.68	1.14	0.39	0.63	0.77	1.29	
	(0.70)	(1.17)	(0.42)	(0.66)	(0.80)	(1.31)	
EA$_{vert}$	0.17	0.63	-0.15	0.15	0.28	0.81	
VDE	1.19	1.67	0.92	1.13	1.28	1.78	
***E*-2-fluorovinyl radical**							
EA$_{ad}$ 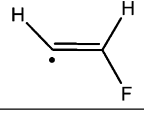	1.51	1.96	1.2	1.48	1.6	2.15	
	(1.54)	(2.00)	(1.23)	(1.52)	(1.63)	(2.18)	
EA$_{vert}$	1	1.45	0.67	0.99	1.1	1.69	
VDE	2.09	2.55	1.78	2.06	2.17	2.68	
***Z*-2-fluorovinyl radical**							
EA$_{ad}$ 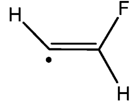	1.59	2.03	1.25	1.61	1.7	2.22	
	(1.63)	(2.07)	(1.28)	(1.66)	(1.75)	(2.25)	
EA$_{vert}$	1.01	1.45	0.66	1.02	1.11	1.69	
VDE	2.27	2.71	1.89	2.39	2.43	2.86	
1-fluorovinyl radical							
EA$_{ad}$ 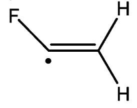	1.55	1.97	1.29	1.5	1.57	2.03	
	(1.59)	(2.01)	(1.34)	(1.54)	(1.62)	(2.07)	
EA$_{vert}$	0.85	1.26	0.54	0.84	0.91	1.42	
VDE	2.26	2.68	2.02	2.18	2.25	2.64	
***Z*-1,2-difluorovinyl radical**							
EA$_{ad}$ 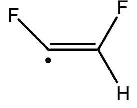	2.07	2.49	1.83	2.01	2.08	2.53	
	(2.13)	(2.55)	(1.88)	(2.07)	(2.14)	(2.58)	
EA$_{vert}$	1.36	1.78	1.08	1.33	1.4	1.89	
VDE	2.77	3.19	2.54	2.7	2.76	3.15	
***E*-1,2-difluorovinyl radical**							
EA$_{ad}$ 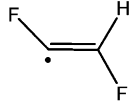	2.06	2.47	1.82	1.99	2.05	2.51	
	(2.11)	(2.52)	(1.87)	(2.04)	(2.10)	(2.55)	
EA$_{vert}$	1.41	1.82	1.13	1.38	1.44	1.97	
VDE	2.76	3.16	2.53	2.67	2.72	3.08	
2,2-difluorovinyl radical							
EA$_{ad}$ 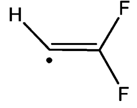	1.96	2.41	1.66	1.93	2.03	2.58	
	(1.99)	(2.45)	(1.69)	(1.96)	(2.07)	(2.60)	
EA$_{vert}$	1.32	1.77	1.01	1.29	1.39	1.97	
VDE	2.65	3.11	2.33	2.63	2.74	3.24	
trifluorovinyl radical							2.1 ± 0.2[b]
EA$_{ad}$	2.43	2.84	2.2	2.35	2.41	2.85	
	(2.48)	(2.90)	(2.25)	(2.40)	(2.46)	(2.90)	
EA$_{vert}$	1.67	2.08	1.42	1.61	1.67	2.17	
VDE	3.17	3.58	2.95	3.09	3.14	3.51	

[a] Ref 43. [b] Ref 48.

was to observe trends in EAs with the inclusion of additional fluorine atoms, and to analyze relative stabilities of the isomers of the mono- and di-fluorinated structures.

All of the optimized structures are predicted to have C_s symmetry and the neutral radicals all have $^2A'$ ground electronic states, i.e. they are σ radicals. These findings are in agreement with previous electron spin resonance (ESR) studies,[6,10−13] which have shown this to be the case for both the vinyl radical and the trifluorovinyl radical. All of the anions have $^1A'$ electronic ground states. Although we were unable to find experimental geometrical data for the substituted vinyl radicals, some studies have suggested that the BHLYP method is the most accurate of the six functionals used here in the optimization of molecular geometry,[22,38−42] while others prefer the B3LYP method.

A. C_2H_3. We found two experimental EAs of the vinyl radical: 0.668 ± 0.024[43] and 0.80 ± 0.2 eV.[44] Comparison of the former of these values with the theoretical results, shown in Table 1, reveals that the B3LYP, BLYP, and BP86 functionals, which yield ZPVE corrected EA$_{ad}$ values of 0.70, 0.66, and 0.80 eV, respectively, predict this EA most accurately, as expected.[2] The geometries of the neutral and anionic species are shown in Figure 1. The BHLYP functional predicts bond lengths and angles in excellent agreement with experiment,[45] although these comparisons should be made with caution since we are comparing a computed r_e geometry with an experimentally derived r_0 structure. The bond lengths (Å) predicted by BHLYP (with corresponding experimental data[45] in parentheses) are 1.078 (1.080 ± 0.010), 1.310 (1.3160 ± 0.0063), 1.083 (1.085 ± 0.010), and 1.088 (1.085 ± 0.010). It should be noted that these last two values represent the two C_β−H bonds, which appear to be equivalent on typical experimental time-scales, i.e. the radical appears to have C_{2v} symmetry due to the rapid rocking-tunneling of the α-hydrogen between equivalent sites. The BHLYP (and experimental) bond angles are 137.2° (137.3 ± 4.0°), 121.4° (121.5 ± 1.0°), and 116.8° (117.0 ± 2.0°). All of the functionals predicted the angles within experimental error and, with the exception of the C_β−H bonds, B3LYP and B3P86 predict the bond lengths within experimental uncertainty. All of the functionals predict longer C−H bond lengths and a marginally longer C═C bond in the anion, relative to the neutral.

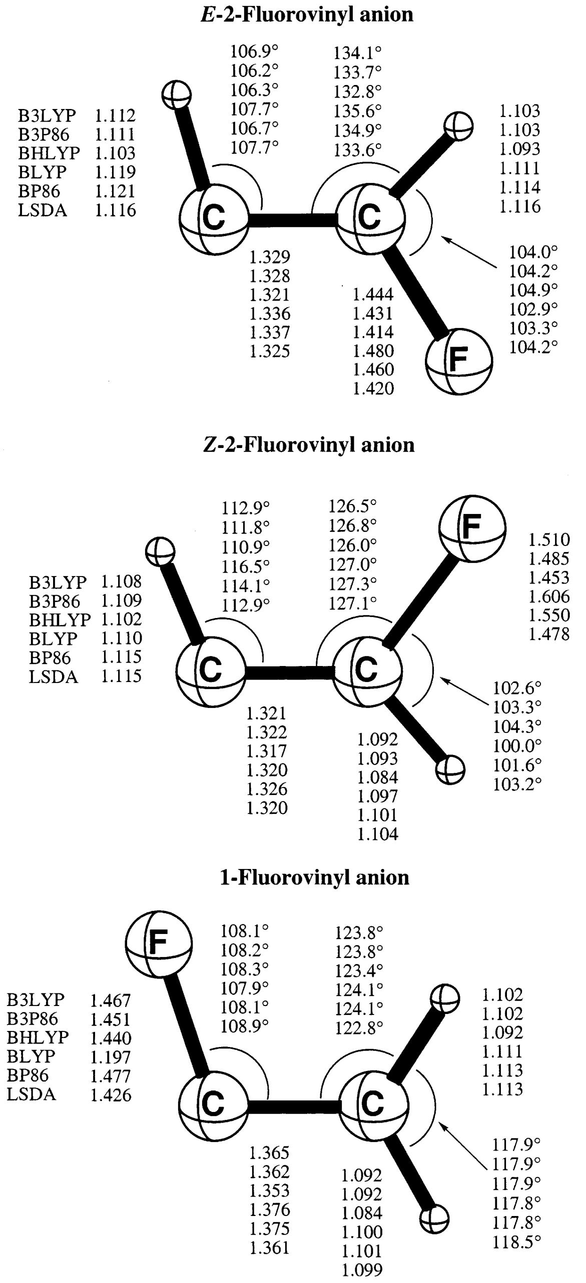

***E*-2-Fluorovinyl anion**

***Z*-2-Fluorovinyl anion**

1-Fluorovinyl anion

Figure 3. $C_2H_2F^-$ bond lengths (Å) and angles.

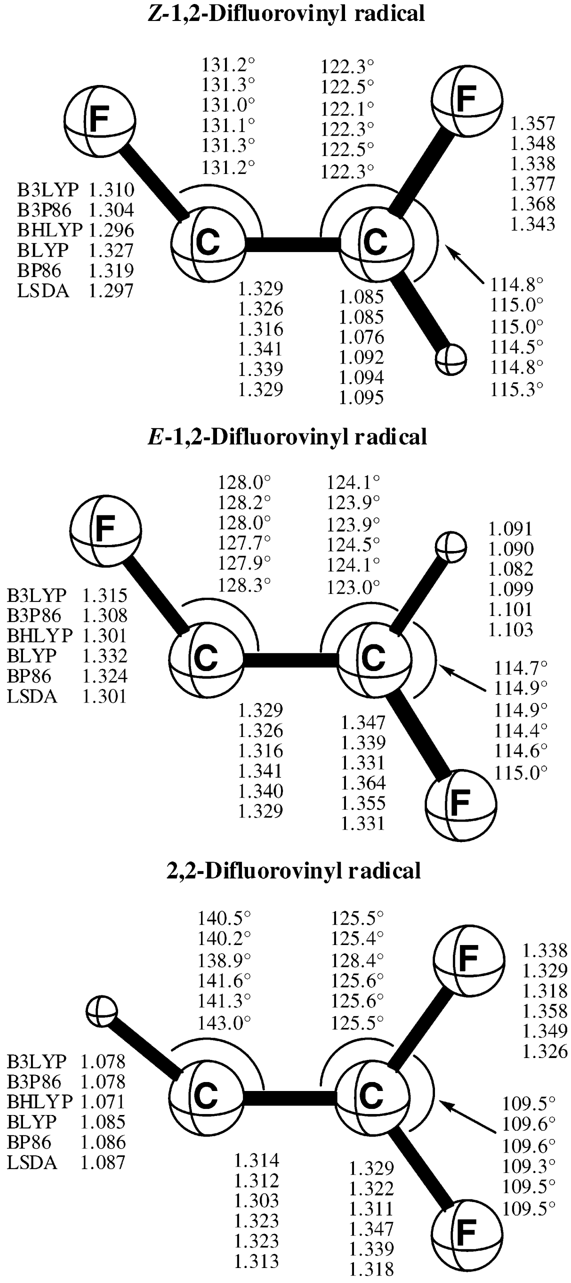

***Z*-1,2-Difluorovinyl radical**

***E*-1,2-Difluorovinyl radical**

2,2-Difluorovinyl radical

Figure 4. C_2HF_2 bond lengths (Å) and angles.

The C−C−H bond angle, centered on the α-carbon, shows a reduction of roughly 30° upon addition of the extra electron, due to the extra repulsion.

B. C_2H_2F. Three isomers of the fluorovinyl radical and anion, whose structures are shown in Figures 2 and 3, were studied. The relative energies of these isomers are presented in Table 2. These values indicate that, of the three isomers, the 1-fluoro species is the most stable for both the neutral and the anion, a result that can be attributed to the ability of the electronegative fluorine atom to inductively withdraw electron density from the α-carbon.

Additional stabilization of the radical results from π donation from fluorine, a weak π donor. The 2-fluorovinyl radicals are roughly isoenergetic, with the *E*-isomer slightly more stable, suggesting that the radical stabilization is dominated by a combination of σ withdrawal and π donation by the fluorine atom at the α-carbon, not resonance. Of the two 2-fluorovinyl anion isomers, the *Z*-isomer is more stabilized with respect to its *E* analogue due to negative hyperconjugation,[46] with DFT predicting the stabilization of the *Z*-2-fluorovinyl anion to fall between 1 and 3 kcal mol^{-1} relative to the *E*-2-fluorovinyl anion.

A vinylic anion exhibiting negative hyperconjugation would be expected to have a shorter carbon−carbon bond length, due to the increase in acetylenic character. However, somewhat paradoxically, all of the DFT functionals predict an increase in this bond length with formation of the anion. Despite this, some increased acetylenic character is evident from the ca. 0.1 Å increase in the C−F bond length in the *Z*-2-fluorovinyl anion, compared to its neutral counterpart.

The B3LYP NPA computation predicts that the fluorine atom has a natural charge of −0.38 in the radical and −0.54 in the anion for the *Z*-isomer. This difference is less pronounced (−0.37 in the radical and −0.49 in the anion) in the *E*-isomer. This increase in negative charge is indicative of a contribution from H−C≡C−H + F$^-$. These hyperconjugative effects are more prevalent in the *Z*-2-isomer than the *E*-2-isomer due to the increased overlap of the nonbonding lone pair (*n*) orbital with the $\pi^*_{\mathrm{C-F}}$ orbital[47] in the antiperiplanar arrangement,

TABLE 2: Energies (kcal mol^{-1}) of the Different Isomers, Relative to the Most Stable Isomer for Each Species (ZPVE corrected values are in parentheses.)

	B3LYP	B3P86	BHLYP	BLYP	BP86	LSDA
E-2-fluorovinyl radical	3.34	3.58	2.54	3.87	4.15	5.16
	(2.94)	(3.21)	(2.24)	(3.38)	(3.69)	(4.67)
Z-2-fluorovinyl radical	3.39	3.72	2.76	3.72	4.11	5.52
	(3.09)	(3.44)	(2.54)	(3.35)	(3.77)	(5.12)
1-fluorovinyl radical	0.00	0.00	0.00	0.00	0.00	0.00
	(0.00)	(0.00)	(0.00)	(0.00)	(0.00)	(0.00)
E-2-fluorovinyl anion	20.3	18.4	19.2	21.1	18.9	15.1
	(23.2)	(21.0)	(21.6)	(23.5)	(21.3)	(17.2)
Z-2-fluorovinyl anion	18.5	16.9	18.4	18.0	16.4	13.9
	(21.4)	(19.4)	(20.7)	(20.2)	(18.7)	(15.9)
1-fluorovinyl anion	16.0	14.8	14.6	17.0	15.4	12.8
	(19.1)	(17.4)	(17.0)	(19.5)	(17.9)	(15.0)
$[\mathrm{F}\cdots\mathrm{H{-}C{\equiv}C{-}H}]^-$	0.00	0.00	0.00	0.00	0.00	0.00
	(0.00)	(0.00)	(0.00)	(0.00)	(0.00)	(0.00)
Z-1,2-difluorovinyl radical	5.62	6.08	6.93	4.56	5.1	5.77
	(6.36)	(6.82)	(7.65)	(5.31)	(5.84)	(6.54)
E-1,2-difluorovinyl radical	6.24	6.69	7.33	5.43	5.93	6.21
	(6.64)	(7.08)	(7.69)	(5.84)	(6.33)	(6.64)
2,2-difluorovinyl radical	0.00	0.00	0.00	0.00	0.00	0.00
	(0.00)	(0.00)	(0.00)	(0.00)	(0.00)	(0.00)
Z-1,2-difluorovinyl anion	3.00	4.24	3.03	2.61	3.97	6.78
	(3.28)	(4.50)	(3.28)	(2.88)	(4.22)	(7.04)
E-1,2-difluorovinyl anion	3.93	5.39	3.65	3.97	5.58	7.73
	(3.92)	(5.35)	(3.58)	(4.02)	(5.57)	(7.73)
2,2-difluorovinyl anion	0.00	0.00	0.00	0.00	0.00	0.00
	(0.00)	(0.00)	(0.00)	(0.00)	(0.00)	(0.00)
$[\mathrm{F}\cdots\mathrm{H{-}C{\equiv}C{-}F}]^-$	2.46	4.21	4.21	1.23	3.02	7.09
	(0.23)	(2.08)	(2.32)	(−1.17)	(0.89)	(5.11)
$[\mathrm{F}\cdots\mathrm{F{-}C{\equiv}C{-}F}]^-$	29.2	33.3	31.6	26.6	31.2	39.7
	(28.1)	(32.2)	(30.5)	(25.5)	(30.0)	(38.4)
trifluorovinyl anion	0.00	0.00	0.00	0.00	0.00	0.00
	(0.00)	(0.00)	(0.00)	(0.00)	(0.00)	(0.00)
$[\mathrm{F}\cdots\mathrm{F{-}C{\equiv}C{-}F}]^-$	50.3	53.3	53.7	47.1	50.4	56.5
	(49.3)	(52.2)	(52.8)	(45.8)	(48.9)	(55.1)

compared with the synperiplanar arrangement. Stabilization of the fluorovinyl radical through effects at the α-carbon is dominant over resonance stabilization. With the exception of BP86 and LSDA, these stabilizing effects are more pronounced in the anion than in the neutral radical.

Computed EAs for the fluorovinyl radical isomers are roughly equal, with DFT consistently predicting the EA of the *E*-2-fluorovinyl radical as the smallest. All the functionals except BHLYP give the EA of *Z*-2-fluorovinyl radical as slightly larger than that of 1-fluorovinyl radical.

C. C_2HF_2. As with the mono-fluorinated structures, there are three isomers to be considered for the difluorinated species. The geometries of these are shown in Figures 4 and 5. The relative stabilities of the different isomers are shown in Table 2, and seem to follow a different pattern than the fluorovinyl species. As with the fluorovinyl radical, the *E*- and *Z*-1,2-difluorovinyl radicals are roughly isoenergetic, with the *E*-1,2-difluorovinyl radical slightly more stable than the *Z*-isomer. The 2,2-difluorovinyl radical is stabilized with respect to the 1,2-difluorovinyl radical by between 5 and 7 kcal mol^{-1}, suggesting that in this case resonant effects are the dominant stabilizing factor, in contrast to the case of mono-fluorinated vinyl radicals.

For the difluorinated anions, the same trend is observed, with the *E*- and *Z*-1,2-difluorovinyl anion energy separation enhanced and the inductive effects seemingly muted. The 2,2-difluorovinyl anion is predicted to lie lower than *Z*-1,2-difluorovinyl by ∼3−4 kcal mol^{-1}, which in turn lies below the *E*-1,2-isomer by ∼0.5−1 kcal mol^{-1}. The electron affinities, shown in Table 1, fit the general trend established in this work, i.e., the presence of the second fluorine increases the electron affinity. There are no experimental EAs for either the mono- or di-substituted radicals, so we are unable to provide an analysis of performance of individual DFT functionals. However, we expect the B3LYP, BLYP, and BP86 EAs to be very reliable.

D. C_2F_3. Spyrou, Sauers and Christopherou report the experimental EA of trifluorovinyl radical as 2.1 ± 0.2 eV.[48] In contrast to the unsubstituted radical, only the BHLYP value (2.25 eV) is within the experimental error—all of the other methods exceed the experimental value. It seems likely that 2.3 eV (the experimental upper bound) is a far more plausible EA for C_2F_3 than is 1.9 eV (the experimental lower bound). Geometrically, the trifluorinated system behaves similarly to its unsubstituted parent upon addition of an extra electron. The structures of the radical and anion are shown in Figure 6. The F−C−C bond angle, centered on the α-carbon closes by approximately 20° upon anion formation. Further evidence of negative hyperconjugation comes from the increase of the anion's C−F bond, anti to the lone pair orbital, by ca. 0.05 Å relative to the neutral radical. A lengthening of slightly smaller magnitude is predicted for the C−F bond syn to the lone pair. The C═C bond length in the vinyl anion is predicted to be 0.02 Å longer than the equivalent bond in the trifluorovinyl anion, indicating that more negative hyperconjucation is afforded by the fluorine substituents than the hydrogens, as expected.

E. Alternative Structures. Some important alternative structures for the fluorinated anions have been characterized—these are shown in Figure 7. These fluoride···acetylene complexes all possess $C_{\infty v}$ symmetry and have a $^1\Sigma^+$ electronic ground state. Our results show that $[\mathrm{F}\cdots\mathrm{H{-}C{\equiv}C{-}H}]^-$ lies lower by ∼15 kcal mol^{-1} with respect to the 1-fluorovinyl anion.

Z-1,2-Difluorovinyl anion

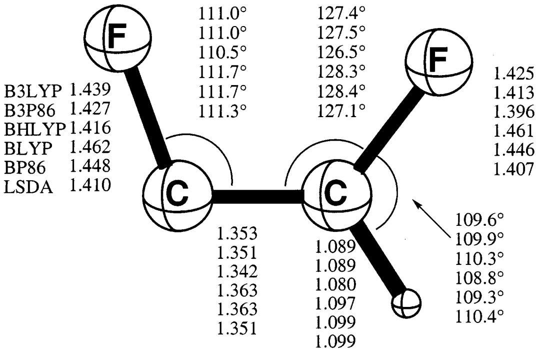

E-1,2-Difluorovinyl anion

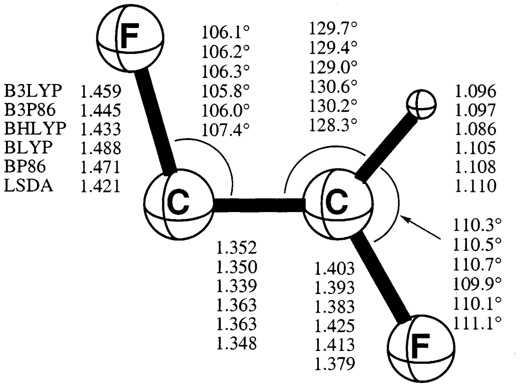

2,2-Difluorovinyl anion

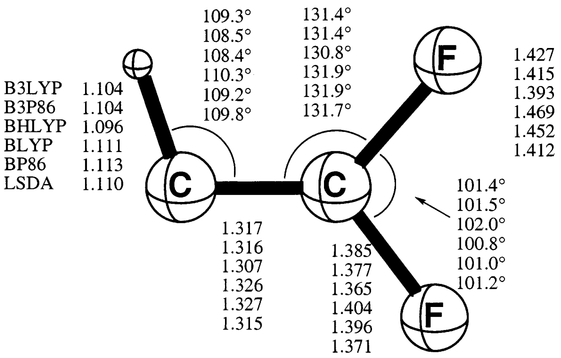

Figure 5. $C_2H_2HF^-$ bond lengths (Å) and angles.

This value increases to ~18 kcal mol^{-1} with the inclusion of ZPVE correction. This complex has been characterized experimentally[49] and theoretically[50] in recent years, yet no energetic comparison has been made between the anionic F···acetylene complex and the fluorovinyl anion. Botschwina, Dutoi, Mladenovic, Oswald, Schmatz, and Stoll[50] have computed the equilibrium dissociation energy (for dissociation to F$^-$ and acetylene) as 24.1 kcal mol^{-1} using the aug-cc-pVQZ CCSD(T) method. Of the difluoro-isomers, only the[F···H−C≡C−F]$^-$ structure is stabilized relative to the vinyl structures discussed previously—this isomer is of comparable energy to the 2,2-difluorovinyl anion with ZPVE taken into account, and ~2 kcal mol^{-1} higher neglecting the ZPVE correction. The BHLYP predicted H−F bond lengths in [F···H−C≡C−H]$^-$ and [F···H−C≡C−F]$^-$, 1.065 and 1.041 Å, are not terribly longer than the equilibrium bond distance of free HF (0.917 Å).[51] This strong H−F bond is responsible for the relatively low energy of these two complexes. The other two linear isomers investigated, [F···F−C≡C−H]$^-$ and [F···F−C≡C−F]$^-$, were found to be significantly higher in energy than the aforementioned C_s structures. These structures also each have a pair of small (~30 cm^{-1}) degenerate vibrational frequencies, making the definitive assignment of these structures as minima on the potential energy surface difficult. The weak F···F interaction, evident from the large separation, does not afford the same stabilization as the F−H hydrogen bond. None of the linear isomers has been considered in the calculation of EAs because of the change in geometry and connectivity that would have to occur between the neutral C_s species and the $C_{\infty v}$ anion.

Trifluorovinyl radical

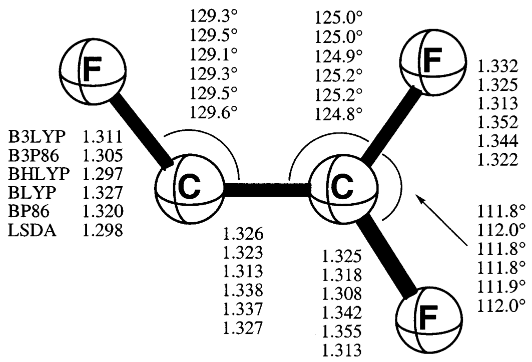

Trifluorovinyl anion

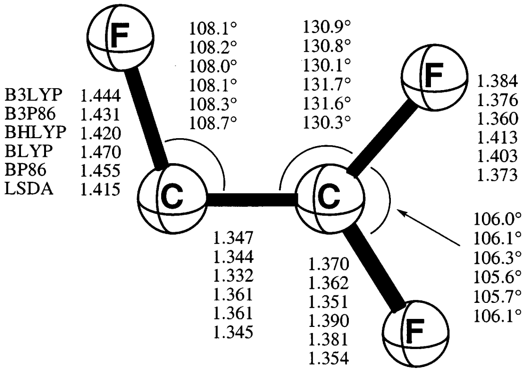

Figure 6. C_2F_3 and $C_2F_3^-$ bond lengths (Å) and angles.

IV. Conclusions

The EAs shown in Table 1 reveal that the vinyl radical EAs increase with the degree of fluorine substitution, due to the ability of fluorine to preferentially stabilize the anion, a trend that was also observed in fluorine-substituted methyl radical EAs.[22]

We have shown that the different isomers of the mono- and di-fluorinated radicals have somewhat different EAs, mainly due to the varying stereoelectronic effects observed in each case. These differences in EA should be analyzed with caution, however, due to the intrinsic uncertainty of the DFT computations. It has been shown that the B3LYP, BLYP, and BP86 methods predict EAs of systems having a closed-shell anion and an open-shell radical to 0.12 eV or better,[22] which is greater than the EA differences between isomers. However, the relative ordering is consistently predicted by all six functionals, allowing us to draw qualitative conclusions.

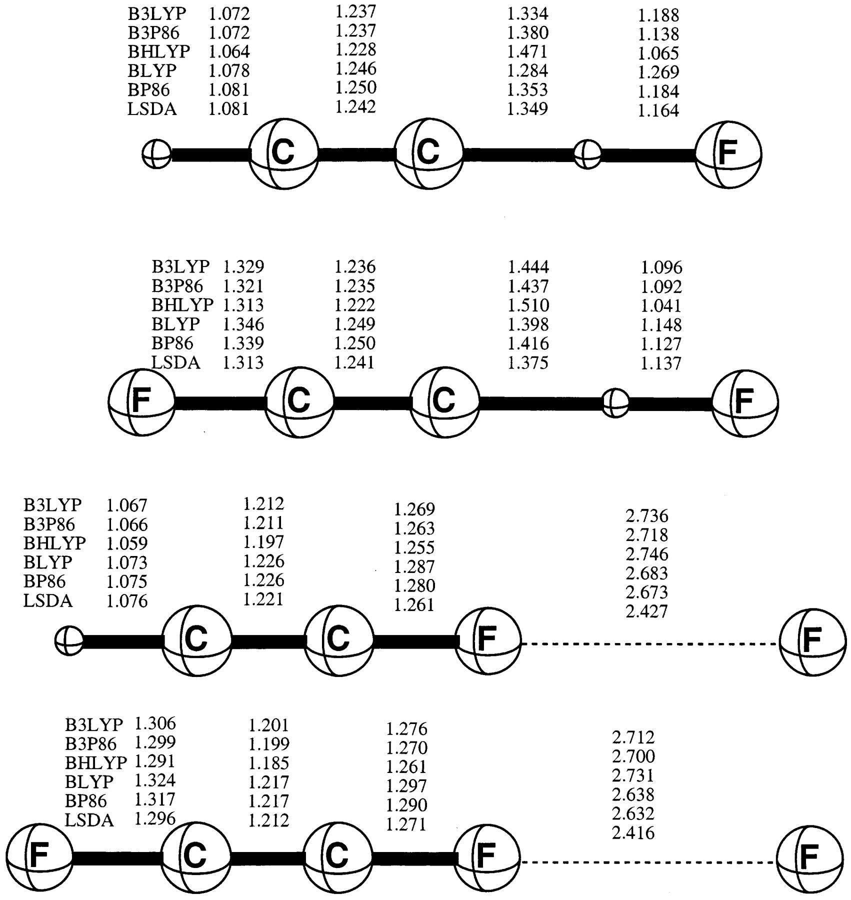

Figure 7. Bond lengths (Å) of the alternative linear anion structures.

Successive substitution of fluorine for hydrogen atoms in the vinyl radical results in a gradual increase in electron affinities. Relative stabilities of isomers of mono- and di-fluorinated vinyl radicals are governed by a competition of electronic effects at the α-carbon and resonance effects. For the monofluorinated anion, inductive withdrawal effects are the dominant stabilizing mode, with some contribution from negative hyperconjugation. In contrast, the radical stability is governed by π donation and σ withdrawal at the α-carbon, with resonance effects relatively minor. For the difluorovinyl radical and anion, however, resonance effects are the major means of stabilization, especially for the radical.

Linear anionic complexes with the same stoichiometry as the fluorinated vinyl radicals were characterized. The fluoride···acetylene complex was found to be considerably more stable than any of the fluorovinyl anions, while the $[\mathrm{F\cdots H{-}C{\equiv}C{-}F}]^-$ complex is of comparable energy to the difluorovinyl anions. The other two linear complexes investigated, $[\mathrm{F\cdots F{-}C{\equiv}C{-}H}]^-$ and $[\mathrm{F\cdots F{-}C{\equiv}C{-}F}]^-$, lie above the corresponding vinylic anions.

Though we do not have enough experimental data to make any meaningful statements about the accuracy of the different methods employed in this work, the relative values of the predicted EAs consistently follow the order:

$$\mathrm{LSDA} > \mathrm{B3P86} > \mathrm{BP86} \geq \mathrm{B3LYP} \geq \mathrm{BLYP} > \mathrm{BHLYP}$$

This is in good agreement with previous studies. Our limited comparison of bond lengths seems to show that BHLYP is the most accurate of the six functionals tested here; however, the B3LYP and B3P86 methods were also found to perform extremely well.

Acknowledgment. We thank Professor Paul Schleyer for his useful suggestions and J. M. Pristera for assistance obtaining published experimental structures. A.C.S. also thanks all of the staff at the CCC. This work was supported by the National Science Foundation, Grant CHE-0136186.

Supporting Information Available: Vinyl radical and fluorinated vinyl radicals and corresponding anions: B3LYP harmonic vibrational frequencies and IR intensities (5 tables). This material is available free of charge via the Internet at http://pubs.acs.org.

References and Notes

(1) Goldschleger, I. U.; Akimov, A. V.; Misochko, E. Y.; Wright, C. A. *J. Mol. Spec.* **2001**, *205*, 269.
(2) Rienstra-Kiracofe, J. C.; Tschumper, G. S.; Schaefer, H. F. *Chem. Rev.* **2002**, *102*, 231.
(3) Paddon-Row: M. N.; Pople, J. A. *J. Phys. Chem.* **1985**, *89*, 2768.
(4) Zhang, P.; Morokuma, K. *Chem. Phys. Lett.* **2003**, *367*, 482.
(5) Lathan, W. A.; Hehre, W. J.; Pople, J. A. *J. Am. Chem. Soc.* **1971**, *93*, 808.
(6) Kasai, P. H. *J. Phys. Chem.* **1986**, *90*, 5034.
(7) Jacox, M. E. *Chem. Phys.* **1980**, *53*, 307.
(8) Wurfel, B. E.; Pugliano, N.; Bradforth, S. E.; Saykally, R. J.; Pimentel, G. C. *J. Phys. Chem.* **1991**, *95*, 2932.
(9) Wurfel, B. E.; Thoma, A.; Bondybey, V. E. *Chem. Phys. Lett.* **1992**, *198*, 135.
(10) Kasai, P. H.; Whipple, E. B. *J. Am. Chem. Soc.* **1967**, *89*, 1033.
(11) Kasai, P. H. *J. Am. Chem. Soc.* **1972**, *94*, 5950.
(12) Cochran, E. L.; Adrian, F. J.; Bowers, V. A. *J. Chem. Phys.* **1964**, *40*, 213.
(13) Fessenden, R. W.; Schuler, R. H. *J. Chem. Phys.* **1963**, *39*, 2147.
(14) Pittmann, C. U.; Kispert, L. D.; Patterson, T. B. *J. Phys. Chem.* **1973**, *77*, 494.
(15) Broadus, K. M.; Kass, S. R. *J. Am. Chem. Soc.* **2000**, *122*, 10697.
(16) Broadus, K. M.; Kass, S. R. *J. Am. Chem. Soc.* **2001**, *123*, 4189.

(17) Kenttämaa, H. *J. Chem. Soc., Perkin Trans. 2* **1999**, 2233.

(18) Damrauer, R.; Hankin, J. A. *Chem. Rev.* **1995**, *95*, 1137.

(19) Cohen, R.; Zenou, N.; Cahen, D.; Yitzchaik, S. *Chem. Phys. Lett.* **1997**, *279*, 270.

(20) Eichkorn, K.; Ahlrichs, R. *Chem. Rev. Lett.* **1998**, *288*, 235.

(21) Taylor, T. R.; Asmis, K. R.; Xu, C.; Neumark, D. M. *Chem. Phys. Lett.* **1999**, *297*, 133.

(22) Li, Q.-S.; Zhao, J.-F.; Xie, Y.; Schaefer, H. F. *Mol. Phys.* **2002**, *100*, 3615.

(23) Huzinaga, S. J. *J. Chem. Phys.* **1965**, *42*, 1293.

(24) Dunning, T. H. *J. Chem. Phys.* **1970**, *53*, 2823.

(25) Pople, J. A.; Gill, P. M. W.; Handy, N. C. *Int. J. Quantum Chem.* **1995**, *56*, 303.

(26) Becke, A. D. *J. Chem. Phys.* **1993**, *98*, 5648.

(27) Lee, C.; Yang, W.; Parr, R. G. *Phys. Rev. B* **1988**, *37*, 785.

(28) Perdew, J. P. *Phys. Rev. B* **1986**, *33*, 8822.

(29) Perdew, J. P. *Phys. Rev. B* **1986**, *34*, 7042.

(30) Becke, A. D. *J. Chem. Phys.* **1993**, *98*, 1372.

(31) In the Gaussian 94 program the BHLYP functional has the formulation $0.5\text{Ex}(\text{LSDA}) + 0.5\text{Ex}(\text{HF}) + 0.5\Delta\text{Ex}(\text{B88}) + \text{Ec}(\text{LYP})$, which differs slightly from Becke's original expression.

(32) Becke, A. D. *Phys. Rev. A* **1988**, *38*, 3098.

(33) Kohn, P. H. a. W. *Phys. Rev. B* **1964**, *136*, 864.

(34) Kohn, W.; Sham, L. J. *Phys. Rev. A* **1965**, *140*, 1133.

(35) Slater, J. C. *Quantum Theory of Molecules and Solids: The Self-Consistent Field for Molecules and Solids*; McGraw-Hill: New York, 1974; Vol. IV.

(36) Vosko, S. H.; Wilk, L.; Nusair, M. *Can. J. Phys.* **1980**, *58*, 1200.

(37) Frisch, M. J.; Trucks, G. W.; Schlegel, H. B.; Gill, P. M. W.; Johnson, B. G.; Robb, M. A.; Cheeseman, J. R.; Keith, T.; Petersson, G. A.; Montgomery, J. A.; Raghavachari, K.; Al-Laham, M. A.; Zakrzewski, V. G.; Ortiz, J. V.; Foresman, J. B.; Cioslowski, J.; Stefanov, B. B.; Nanayakkara, A.; Challacombe, M.; Peng, C. Y.; Ayala, P. Y.; Chen, W.; Wong, M. W.; Andres, J. L.; Replogle, E. S.; Gomperts, R.; Martin, R. L.; Fox, D. J.; Binkley, J. S.; Defrees, D. J.; Baker, J.; Stewart, J. P.; Head-Gordon, M.; Gonzalez, C.; Pople, J. A. Gaussian 94, Revision E.2; Gaussian, Inc.: Pittsburgh, PA, 1995.

(38) Pak, C.; Rienstra-Kiracofe, J. C.; Schaefer, H. F. *J. Phys. Chem.* **2000**, *104*, 11232.

(39) Pak, C.; Xie, Y.; Huis, T. J. V.; Schaefer, H. F. *J. Am. Chem. Soc.* **1998**, *120*, 11115.

(40) Li, Q.; Xu, W.; Xie, Y.; Schaefer, H. F. *J. Phys. Chem.* **1999**, *103*, 7496.

(41) King, R. A.; Mastryukov, V. S.; Schaefer, H. F. *J. Chem. Phys.* **1996**, *105*, 6880.

(42) Pak, C.; Xie, Y.; Schaefer, H. F. *Mol. Phys.* **2003**, *101*, 211.

(43) Ervin, K. M.; Gronert, S.; Barlow, S. E.; Gilles, M. K.; Harrison, A. G.; Bierbaum, V. M.; DePuy, C. H.; Lineberger, W. C.; Ellison, G. B. *J. Am. Chem. Soc.* **1990**, *112*, 5750.

(44) Lias, S. G.; Bartmess, J. E.; Liebman, J. E.; Holmes, J. L.; Levin, R. D.; Mallard, W. G. *J. Phys. Chem. Ref. Data Suppl. No. 1* **1988**, 17.

(45) Kanamori, H.; Endo, Y.; Hirota, E. *J. Chem. Phys.* **1990**, *92*, 197.

(46) Schleyer, P. v. R.; Kos, A. J. *Tetrahedron* **1983**, *39*, 1141.

(47) The C−F antibonding orbital is often referred to as a σ^* orbital. This controversy is addressed by Schleyer and Kos[46] and references therein.

(48) Spyrou, S. M.; Sauers, I.; Christophorou, L. G. *J. Chem. Phys.* **1983**, *78*, 7200.

(49) Jeng, M.-L. H.; Ault, B. S. *J. Phys. Chem.* **1991**, *95*, 2687.

(50) Botschwina, P.; Dutoi, T.; Mladenovic, M.; Oswald, R.; Schmatz, S.; Stoll, H. *Faraday Discuss.* **2001**, *118*, 433.

(51) Huber, K. P.; Herzberg, G. *Molecular Spectra and Molecular Structure IV: Constants of Diatomic Molecules*; Van Nostrand Reinhold: New York, 1979.